Metabolic and transcriptional responses of glycerolipid pathways to a perturbation of glycerol 3-phosphate metabolism in Arabidopsis

Shen, Wenyun; Li, John Qiang; Dauk, Melanie; Huang, Yi; Periappuram, Cyril; Wei, Yangdou; Zou, Jitao

Publisher's version / Version de l'éditeur:
https://doi.org/10.1074/jbc.M109.097758
The Journal of Biological Chemistry, 285, 30, pp. 22957-22965, 2010-03-19

Metabolic and transcriptional responses of glycerolipid pathways to perturbation of glycerol-3-phosphate in Arabidopsis

Wenyun Shen[‡], John Qiang Li[‡ §], Melanie Dauk[‡], Yi Huang[‡], Cyril Periappuram[‡], Yangdou Wei[§] and Jitao Zou[‡ 1]

From the [‡] Plant Biotechnology Institute, National Research Council Canada, Saskatoon, Saskatchewan S7N OW9, and the [§] Department of Biology, University of Saskatchewan, Saskatoon, Saskatchewan S7N 5E2, Canada

Abstract

In the leaf cells of Arabidopsis, glycerolipid synthesis involves two major metabolic pathways compartmentalized in the chloroplasts and cytosol, respectively. Although the operations of these two parallel pathways are regulated with considerable flexibility, the factors mediating this process remain unclear. To investigate the role of glyceorol-3-phosphate (G-3-P) in influencing the interactions of the two glycerolipid pathways, we generated Arabidopsis transgenic lines with a feedback resistance G-3-P dehydrogease gene *gpsA*^{fr} from *E. coli.* The gpsA^{fr} was detected in the cytosol, but augmented G-3-P levels were observed in the cytosol as well as in chloroplasts of the transgenic lines. Results of glycerolipid composition and fatty acid positional distribution analysis illustrated an altered fatty acid flux sharing that affected not only the molar ratios of glycerolipid species but also their fatty acid composition. To decipher pathway complexity, a transgenic line was subjected to lipidomic analysis as well as global gene expression survey. Our results revealed that changes in G-3-P metabolism caused altered expression of a broad array of genes. When viewed from the prospective of glycerolipid metabolism, coherent networks emerged, exposing many enzymatic components of the glycerolipid pathways operating in a modular manner under the influence of G-3-P. Thus, although the biochemical machinery defines the details of how the two glycerolipid pathways functions as separated units of underlying biological activities, G-3-P level seems to guide the coordination of many of its components at the transcript level.

Introduction

In plant cells, fatty acids are generated primarily in the plastid, but glycerolipid biosynthesis takes place both in the chloroplasts and in the cytosol (1, 2, 3). The glycerolipid pathway in the chloroplast is believed to be crucial for generating phosphatidylglycerol (PG), but in species such as Arabidopsis, it also contributes partially to the production of monogalactosyldiacylglycerol (MGDG) and digalactosyldiacylglcyerol (DGDG) in the chloroplast. The glycerolipid pathway in the cytosolic compartment, known as the eukaryotic pathway, sustains the synthesis of all membrane phospholipids in the cytosol, and also participates in generating some of the DAG pool required for the synthesis of MGDG and DGDG (3). The chloroplast pathway incorporates fatty acid groups from acyl-ACP to generate glycerolipids with characteristics resembling that of cyanobacteria glycerolipids, i.e., with almost exclusively C_{16} fatty acid esterified at the *sn-2* position (4 - 7), and hence is termed the prokaryotic pathway. Because the *sn-2* C_{16} fatty acid in the MGDG originating from the prokaryotic pathway is subsequently desaturated to form *cis*-7, 10, 13-hexadecatrienoic acid ($C_{16:3}$) (8, 9), the presence of 16:3 is indicative of the contribution from the prokaryotic pathway. Species which possess a significant portion of 16:3 MGDG are generally called 16:3 plants.

In Arabidopsis, a typical 16:3 plant, close to half of the DAG moieties originating from the eukaryotic pathway are channeled to the chloroplast for membrane glycerolipid synthesis (10). However, the flux of the DAG channeling is flexible, often readjusted under different growth conditions (11 - 13), or in the presence of genetic lesions (14 - 19). Understanding this metabolic readjustment is important because impairments in balancing the two glycerolipid pathway have consequences for plant performance (20 - 22).

G-3-P is an obligate precursor for both pathways at the initial and committed step of glycerolipid synthesis. Experiments using isolated chloroplast and leaf explant have all indicated G-3-P as a factor influencing the balance of the glycerolipid pathways (1, 3, 7, 23, 24). A deficiency in the provision of G-3-P within the chloroplast reduced the carbon flux through the prokaryotic pathway (25). In all these studies, the role of G-3-P was explained chiefly by its capacity in affecting the fatty acylation process in the chloroplasts. In this study, we generated transgenic Arabidopsis plants with increased G-3-P levels through over expressing an *E. coli* gene encoding a glycerol-3-phosphate dehydrogenase ($gpsA^{fr}$) which is insensitive to feedback inhibition (26). The transgenic lines had G-3-P level several fold higher than wild type controls

under standard growth conditions. The transgenic plants exhibited glycerolipid phenotype consistent with adjusted metabolic balance between the two glycerolipid pathways when compared with wild type plants. We conducted lipidomic as well as global gene expression analysis. Our data provide a comprehensive view of the metabolic and enzymatic components involved in balancing the two glycerolipid pathways in response to G-3-P level changes. Results from our study also reveal many changes at the transcript level of many enzymatic components of the glycerolipid pathways associated with G-3-P perturbation.

EXPERIMENTAL PROCEDURES

Plant Materials and growth conditions —Plants were grown in growth chambers with a 16 h light and 8 h dark regime with a photosynthetic photon flux density of 75 μmol photons $m^{-2} \cdot s^{-1}$. The day/night temperature was controlled at 22/17°C. All biochemical analyses were performed with leaves harvested at the rosette stage of 3-week-old plants.

Construction of a plant transformation vector for gpsA^{FR} —Bacterial strain BB26-36R2 (*gpsA^{FR}*, *plsB*), was a generous gift from Professor John E Cronan Jr. (University of Illinois, Urbana-Champion). The gpsA allele was PCR amplified and fully sequenced. Primers GAGAGCTCTTAGTGGCTGCTGCGCTC (GPSA31) and GAAGAAGGATCCAACAATGAACCAACGTAA (GPSA5) were designed according to the sequence of *gpsA^{FR}* (accession P37606) with *SacI* and *BamHI* restriction sites, respectively, at each end. The primers were used to perform PCR amplification of the *gpsA^{FR}* sequence. The PCR products were purified with QIAquick PCR purification Kit (Qiagen) and digested with *SacI*/*BamHI*. The *SacI*/*BamHI* digested *gpsA^{FR}* DNA fragment was subsequently inserted into the *Agrobacterium* binary vector pBI121 (Clontech) to replace the GUS gene. The *gpsA^{FR}* gene expression cassette thus contains the *gpsA^{FR}* gene under the control of the constitutive 35S promoter and flanked at the 3' end with the NOS terminator. The junction region between the 35S promoter and the *gpsA^{FR}* encoding sequence was confirmed through sequencing. Transformation of Arabidopsis was performed through vacuum infiltration, and T1 transgenic plants were selected through germinating seed in ½ MS medium containing 50 mg/l kanamycin. Biochemical analysis was performed with tissues harvested from T2 plants.

Chloroplast preparation —Chloroplasts were isolated from 3 week-old Arabidopsis rosette leaves according method of Rensink et al. (1998), using a percoll gradient consisting of 2 mL of 70% (v/v) Percoll (Sigma-Aldrich), 4 mL of 50% (v/v) Percoll, and 4 mL of 40% (v/v) Percoll/grinding buffer in a 15-mL polycarbonate tube. The gradient was centrifuged for 15 min at 5000 rpm in the HB-4 rotor with the brake off. The (lower) band at the 50% to 70% interface was isolated for G-3-P content and western blot analysis. Protein content was measured according to the method of Bradford (42).

Metabolite Extraction and Analysis —G-3-P in leaf tissue was extracted according the method of Shen et al. (35). G-3-P in chloroplast was extracted according the method of Sauer and Heise (39). Ice-cold chloroplast suspensions immediately after isolation were centrifuged through a layer of silicone oil into 20 ul of 1M $HClO_4$. The G-3-P concentration in the neutralized leaf and chloroplast extracts was measured enzymatically via glycerolphosphate dehydrogenase. Inorganic phosphate in leaf tissue was determined by the method of Ames (43).

Fatty Acid and Lipid Analysis —Arabidopsis leaves in 2 ml of 10% KOH in methanol were heated at 80°C for 2 hours. After cooling down to room temperature, addition of 1 ml of 50% HCl, the mixtures were extracted with 2 ml hexane, and dried under N_2. Each sample was then added with 2 ml of 3N methanol- HCl, and heated at 80°C for 2 hours. After addition of 2 ml of 0.9 % NaCl solution and hexane, fatty acid methylesters (FAMES) were extracted into the organic phase, and separated by GC. Lipid extraction and purification by two dimensional TLC on silica gel 60 (EMD chemical, Germany) were performed according the method of Miquel and Browse (18). Lipids were visualized with iodine vapor. Individual lipids were isolated from TLC plates and used to prepare FAMES. The methyl esters were quantified by GC using 17:0 fatty acid as internal standard. Fatty acid composition at the *sn*-2 position of the glycerol backbone was determined by lipase digestion according to Miquel *et al.* (25).

Immunoblot Analysis of gpsA^{FR} Protein from Roots and Leaves — Polyclonal antibodies were raised in rabbits to two polypeptides, GLEAETGRLLQDVAREALGDQIPLAVISGP and LASTDQTFADDLQQLLHCGKSFRVYSNPDF, synthesized based on the deduced amino acid sequence of the *E. coli* gpsA^{FR}. Immunoblot analysis of gpsA^{FR} protein from total leave extracts and purified chloroplast were performed according to Millenaar et al. (2000). Proteins (10ug) were separated by SDS–PAGE, and subsequently electro-transferred to nitrocellulose filters using blot transfer buffer (25 m M Tris, 192 m M glycine, 20% (v/v) methanol). Antiserum for gpsA^{FR} were used as primary antibodies with a dilution factor of 1:1000. Anti-rabbit IgG Fab fragments conjugated to peroxidase (**Boehringer Mannheim, Germany**) were used as a secondary antibody (1:25 000). The blot was detected for 1.5 min using protein gel blotting detection reagent ECL+ Plus (Amersham Pharmacia Biotech) and then developed with Biomax MR film (Kodak).

RNA extraction and Microarray analysis —Total RNA of each tissue was extracted using RNeasy Mini Kit (50) (Qiagen, Mississauga, ON) under the manufacturer's recommendations and subjected to RNase-free DNase I treatment (Invitrogen, Valencia, CA, USA) at 25°C for 15 min to remove contaminating DNA. The yield and RNA purity were determined spectrophotometrically with a spectrophotometer DU@740 (Beckman, USA), and the quality of RNA was verified by electrophoresis on a denaturing formaldehyde agarose gel. Purified total RNA was precipitated and resuspended in DEPC-treated water to a final concentration of about 500 ng/μL.

Synthesis of cDNA, cRNA labeling, hybridization and scanning were performed at the Botany Affymetrix Genechip Facility, University of Toronto (Toronto, ON, Canada). Three independent biological replicates were performed for the wild type and the transgenic line, respectively. A total of six .CEL files containing the raw probe intensity values were imported into the R-package Affy (44). Background adjustment and quantile normalization were performed using the robust multi analysis (RMA) package implemented in Bioconductor (http://www.bioconductor.org/) (31). The quantile normalization method was used because it has better precision than MicroArray Suite 5.0 (Affymetrix) and dChip for low expression values (45). Using the R-package LIMMA (by reading the data and creating an expression set of the data after log 2 transformation), a linear model was fitted and contrast of 'transgenic versus wild-

type' was extracted. For each gene, the mean $\log_2$fold change and corresponding *p*-value was calculated from an empirical Bayes approach which was used to compute moderated *t*-statistics (46), and false discovery rate (FDR) correction (47) was applied to account for testing of multiple genes. Genes were considered to be differentially regulated if the *p*-value was less than 0.05 and the fold change in expression level was great than 1.5. Functional annotation of the genes were obtained from the The Bio-Array Resource for Arabidopsis Functional Genomics database (BAR) (http://bar.utoronto.ca/) by using the probe set numbers provided by the GeneChip manufacturer (Affymetrix Co.).

Real-time quantitative RT-PCR analyses — Total RNA was extracted from leaves of wild type and the transgenic lines, respectively, with the Plant RNeasy Mini kit (QIAGEN, Ontario, Canada). The amount of RNA was determined by spectrophotometry at 260 nm, and its integrity was assessed by gel electrophosis.

For real-time quantitative RT-PCR (real-time qRT-PCR), 1 μg of total RNA was used for cDNA synthesis with QuantiTect Reverse Transcription kit (QIAGEN, Ontario, Canada). Specific primers (Tm, 57°C-63 °C) were designed to generate PCR products between 75-130 bps. The specificity of all primers was checked with BLASTn search (BLAST, http://blast.ncbi.nlm.nih.gov/Blast.cgi). Actin 2 (AT3G18780) was used as an endogenous control for standardization. All primers used for qRT-PCR are listed in Table S5.

Real-time qRT-PCR was performed with Power SYBR Green PCR Master Mix (Applied Biosystems) and amplification was monitored with ABI StepOne Realtime PCR Systems (Applied Biosystem). The standard thermal profile was used for all PCRs: 50 °C for 2 minutes; 95 °C for 10 minutes, followed by 40 cycles of 95 °C for 15 seconds, 57 °C for 30 seconds, 72 °C for 30 seconds. Data acquisition and analysis were done using StepOne software 2.0 (Applied Biosystems). Genes picked for verification with real-time PCR were chosen based on their possible significance in glycerolipid pathways. Results from three replicates were shown.

RESULTS

Transgenic plants using a feedback insensitive E. coli G-3-P dehydrogeasne gene gpsA^{FR} had elevated G-3-P content in both the cytosol and chloroplasts — We took a transgenic approach to increase cellular G-3-P level. Studies of Bell and Cronan (26) discovered a mutant *E. coli* strain, BB26-36R2 (*gpsA^{FR}*, *plsB*), in which the G-3-P auxotrophic phenotype, due to a mutation in G-3-P acyltransferase (*plsB*), is suppressed by a second mutation in the structural gene (*gpsA*, accession P37606) encoding the biosynthetic GPDH. The mutated version of the GPDH, *gpsA^{FR}*, was about 20-fold less sensitive to feedback inhibition, and as a result, *E. coli* strain harboring this allele had G-3-P content 12 times higher than that of the control. We amplified the coding regions of the gpsA^{FR} allele, and revealed a point mutation in the codon for aa$_{255}$ (GAC→GAA), which resulted in a conversion of Asp$_{255}$ in the wild enzyme (PID: g91790037) to Glu$_{255}$ in gpsA^{FR}. The structural significance of this amino acid substitution is unclear, but the residue is located very close to the active site pocket based on the structure of a human GPDH (27). This gpsA^{FR} allele was inserted into a plant transformation vector under the control of the constitutive CaMV 35s promoter, and introduced into *Arabidopsis thaliana* (ecotype *Columbia*).

The *gpsA^{FR}* transgenic plants were indistinguishable from wild type plants in growth and development under standard growth conditions. We examined the presence of gpsA^{FR} protein in several transgenic lines by immunoblot analysis. Total leaf protein extract and protein prepared from purified chloroplast were subjected to SDS-PAGE as described in "Materials and Methods". High level of gpsA^{FR} protein was detected in the total leaf extract, but not from that of the purified chloroplast (**Figure 1a**). Thus, as expected, the *gpsA^{FR}* protein appeared to be localized in the cytosol.

G-3-P content was assessed using rosette leaves of plants growing in soil. Leaf tissues of wild type Arabidopsis plants have G-3-P concentration of 60 nmol/gram fresh weight (FW), while the transgenic lines had G-3-P content at 200 nmol/g FW (**Figure 1b**). From the same batch of plants we then isolated chloroplasts, and determined G-3-P content in this particular compartment. The wild type Arabidopsis chloroplasts under our growth conditions had a G-3-P content at about 5 nmol per micro gram chloroplast (5 nmol/mg chl), a level within the range reported for spinach (11 nmol/mg chl) (1). But chloroplasts of the transgenic lines had a G-3-P level several fold higher than that of the wild type control. The chloroplast G-3-P content might

have been underestimated due to possible leakage during organelle fractionation. Nevertheless, by comparing the wild type plants and the transgenic lines that underwent the same procedure, it became apparent that the G-3-P content in the chloroplast of the transgenic lines was much higher. Thus, consistent with the presence of a chloroplast membrane carrier that is capable of accepting 3-carbon compounds with a phosphate molecule attached to it (28), our finding suggested that G-3-P in the cytosol was likely transported across the chloroplast membrane.

The gpsA^{FR} transgenic plants exhibit altered fatty acid profiles in leaf but have no changes in double bond indices —Survey of total lipid fatty acid profiles in leaves from a large number of transgenic lines consistently showed increased 16:0 and 16:3 contents (data not shown). **Table 1** presents data from some of the selected lines. The molar ratios of $C_{18:1}$, $C_{18:2}$ and $C_{18:3}$ fatty acids were all substantially decreased. Consequently, the general alteration of fatty acid profile in leaf tissue can be best described as an increased ratio of C_{16}/C_{18} fatty acids. Thus, in keeping with chloroplast feeding experiments (1), the increased G-3-P appeared to reduce palmitoyl-ACP elongation *in planta* as well. However, these fatty acid compositional changes do not seem to alter the general membrane unsaturation level based on assessment of double bond indices (29). Further analysis presented below will be focused on two transgenic lines.

The gpsA^{FR} transgenic plants have altered glycerolipid composition in leaves —We separated major glycerolipid species through 2-D TLC, and analyzed their profiles in leaf tissues. The results presented in **Table 2** include several changes. Firstly, substantial increases in 16:0 across all lipid species, but particularly in DGDG and PC, were noticeable. Secondly, the proportion of MGDG was substantially increased, whereas the level of DGDG and the contents of phospholipids molecules particularly PC and PE were reduced. Thirdly, compositions of polyunsaturated fatty acids in galactolipids were modified, with both MGDG and DGDG displaying a lowered $C_{18:3}$; in the case of MGDG, the reduction of $C_{18:3}$ was almost entirely counterbalanced by an increase in $C_{16:3}$, and thus incurred no changes in the content of trienoic; in DGDG, increase in both $C_{16:3}$ and $C_{16:0}$ was detected. Fourthly, both PC and PE in the transgenic lines contained less 18:2, and consequently had an increased 18:3/18:2 ratio in lipids of the eukaryotic pathway origin.

Glycerolipid composition changes resulted from a modified flux to the two glycerolipid pathways —The increased C16:3 and augmented ratio of total 16- and 18-carbon fatty acid in MGDG and DGDG suggested that the prokaryotic glycerolipid pathway was enhanced in the transgenic lines. To verify this, we performed compositional analysis of fatty acid at the *sn*-2 position of MGDG and DGDG. As seen in **Figure 2**, the molar percent of *sn*-2 C-16 fatty acid was significantly higher in MGDG and DGDG of the transgenic lines. Our analysis with PG also showed a similar trend. These results thus confirmed that in the transgenic lines an enhanced G-3-P production was associated with a metabolic readjustment that augmented the relative contribution of the prokaryotic glycerolipid pathways. Based on the firmly established concept that diacylglycerol moiety with a *sn*-2 C-16 fatty acid originates from the prokaryotic pathway (10), we were able to deduce the relative contribution of the two glycerolipid pathways in the transgenic lines. As shown in Table 3, in all three glycerolipid species, the relative contribution from the prokaryotic pathway versus the eukaryotic pathway was increased. Interestingly, our analysis also showed that there was an increased level of C-16 at the *sn*-2 of PC as total PC decreased, suggesting that DAG formed by the prokaryotic pathway may also be channeled back for PC synthesis (17).

Lipidomic analysis reveals molecular species profile changes in all glycerolipid classes — Comparative analysis of individual molecular species within subsets of glycerolipids may shed new light on alterations of lipid metabolism in the *gpsA*^{FR} lines. To this end, a complete lipid compositional profile of rosette leaf tissues of three week old seedlings was generated from a lipidomic analysis performed at the Kansas Lipidomic Research Center (http://www.k-state.edu/lipid/lipidomics/) (30). The analysis, which is based on electronspray tandem mass spectrometry (ESI-MS/MS), yields information on phospholipid and glycolipid molecules to the level of head group and the carbon chain length and degree of unsaturation of the acyl groups. Data presented in Figure 3 were uncorrected for specific response factors of individual molecular species, and the analysis was focused on comparison of relative mol% of the individual glycerolipid species. In both MGDG and DGDG, there was an increase of C34:6 and C34:5, but a decrease in C36:6 and C36:5. Together with the aforementioned *sn*-2 fatty acyl composition analysis, these results further confirmed a reduced channeling of DAG moieties from the

eukaryotic pathway to chloroplast. In PG, the most significant change was the increased C32:1, C32:0, and C34:0. In PC, PE and PI, the changes in the profiles of individual molecular species were particularly similar in one aspect, which is that they were enriched with C34:3. Since lipid species of eukaryotic pathway can only have C16 at the *sn*-1 position, the C34:3 phospholipid species should primarily be C16:0 (*sn*-1)/18:3 (*sn*-2). The increased 16:0/18:3 phospholipids could be caused by an enhanced acylation of 16:0 at the *sn*-1 in the cytosolic pathway, a reduced channeling of this type of DAG to the chloroplast, or the combination of both. Previously, increases in the amount of 16:0 in PC were attributed to enhanced turnover of prokaryotic MGDG, followed by the utilization of the fatty acid for synthesis of other lipids (17).

Inducible effect of altered G-3-P metabolism on networks of gene expression —To investigate a potential regulatory role of G-3-P metabolism in the context of globe gene expression network, we surveyed the transcriptome of three week old rosette leaves using the Affymetrix ATH1 gene chip. To identify genes that were differentially regulated in $gpsA^{FR}$ transgenic plants, the data were preprocessed using the robust multiarray analysis (RMA) for background adjustment and normalization (31). A total of 389 diferentially expressed genes were identified (1.5-fold change cut off; false discovery rate, p value < 0.05) including 78 upgraduated and 311 downregulated (Table S1).

We specifically inspected lipid metabolism genes according to a list compiled at (http://lipids.plantbiology.msu.edu/master_table.htm?q=lipids/genesurvey/master_table.htm), and the microarray data for all of these genes are provided in Table S2. Genes whose expression change reaching 1.5 fold represent only a small portion of lipid metabolism enzyme genes. This is expected since perturbation of transcripts encoding basal components of the biochemical pathways should be small. However, there are a number of genes displaying ratio of expression level significantly deviated from 1 when compared with the wild-type control. A total of 28 glycerolipid biosynthesis related genes were selected according to their significance in the glycerolipid pathways (Table S3) and then mapped onto the biochemical pathways complied from AraCyc database (http://www.arabidopsis.org/biocyc/index.jsp) and publications (2, 32). This unraveled a pattern illustrating a coordinated adjustment of gene expression between enzymes of the two glycerolipid pathways (Figure 4). Many genes involved in the prokaryotic

pathway displayed some degree of enhanced expression, among which the most induced is ACP4, which, in addition to carrying the nascent acyl chains during the synthesis of 16- and 18-carbon acyl groups, also serves as the acyl donor for glycerolipid biosynthesis within the chloroplast. Strikingly, although the plants were raised under identical conditions, the expression of the plastidic desaturase genes, including FAD5 (At…), FAD6 (At…), FAD7 (At…) and FAD8 (At…), were all increased somewhat in the *gpsA*^{FR} line. The transcript levels of the eukaryotic pathway enzyme genes, on the other hand, were mostly reduced. These include the lysophosphotidic acid transferase, LPAAT2 (At3g57650), CDP-DAG synthase (At4g22340), the aminoalcoholphosphotransferase AAPT2, which catalyze the transfer of CDP-choline and CDP-ethanolelamine to *sn*-1, 2 diacylglycerol (DAG) to form PC and PE, and the oleoyl-phosphatidylcholine desaturase FAD2. Furthermore, enzyme genes involved in choline synthesis and activation, including a phosphoethanolamine N-methyltransferase (NMT3), aminoalcoholphosphotransferase (AT1G13560) AAPT1 and choline kinase (At4G09760), were also all suppressed in the *gpsA*^{FR} line.

Exceptions to the contrary mode of changes in the two glycerolipid pathways were also found, but they too were consistent with the lipid phenotype. Transcript of *DGD1*, which mediates the synthesis of DGDG from MGDG in chloroplast, was not increased, but rather decreased substantially. This may in part contributed to a decreased total amount of DGDG in the *gpsA*^{FR} line. We also detected some reduction in the transcript level of beta-ketoacyl-ACP synthase II (KAS II). Since KAS II is involved in fatty acid elongation from 16:0-ACP to 18:0-ACP. (KAS II), its reduction may be relevant to the increased 16/18 ratio of the *gpsA*^{FR} line. In the ER compartment, the FAD3 that generates 18:3 from 18:2 in the PC and PE, exhibited a modest increase in transcript level as opposed to decreased transcript level of FAD2. This may lead to an enhanced conversion of 18:2 to 18:3, thereby explaining the higher 18:3/18:2 ratio detected in PC and PE.

Due to the fact that expression changes of most genes in the glycerolipid pathways are less than 1.5, we have conducted quantitative RT-PCR assay on 17 genes to verify the microarray results (Table S4). The fold change values from both techniques were highly correlated (Pearson correlation value = 0.85) (Figure 5). This result showed good consistency between the two methods and confirms the overall reliability of the microarray data.

DISCUSSION

G-3-P is an intermediary metabolite linking several pathways in the metabolic network (33 - 37). The cellular G-3-P pool may thus be influenced by a multitude of metabolic factors. In comparison to glycerol / G-3-P feeding experiments and mutant studies, transgenic enhancement of G-3-P level offered the advantage of not disrupting the associated regulatory circuit of the metabolic network in plant. The feedback resistant $gpsA^{FR}$ gene appeared to be particularly potent in increasing G-3-P level, because it was recently reported that the overexpression of Gly1, a G-3-P dehydrogenase from Arabidopsis had only wild type-like basal level of G-3-P (38).

Results of glycerolipid analysis from the $gpsA^{FR}$ transgenic lines confirm and extend previous reports that an increased G-3-P level was correlated with an augmented contribution of the prokaryotic pathway. Our work also serves to emphasize that interaction between the two glycerolipid pathways is manifested by the channeling of DAG moiety between the two cellular compartments, but the interface of coordination occur at multiple metabolic junctures. This is exemplified by the potential channeling of DAG moieties from the chloroplast to PC synthesis. Consequently, balance adjustment between the two glycerolipid pathways also has broad impact on the distribution of individual molecule species within each subset of glycerolipids. In this regard, we detected a slightly but appreciable increase of *sn*-2 C16 in PC, and a larger representation of C16/C18 DAG moiety in phospholipids. While the increase of *sn*-2 C16 PC species is likely caused by a two-way exchange of lipids between the chloroplast and the ER (18), the preferential incorporation of C16 fatty acids in eukaryotic pathway lipids may be attributed in part to an enhanced turnover of prokaryotic MGDG, followed by the utilization of the fatty acids for synthesis of other lipids (17). Significant transfer of acyl groups from the chloroplast to the extrachloroplast membranes have been documented in *fad7* (*fadD*) (14) and *fad6* (*fadC*) mutant (16).

A metabolic network is often studied as a system downstream of the control from the transcriptome. How an intermediary metabolite can serves as a signal of gene expression affecting the regulatory architecture of the transcription network has been rarely studied. Previous studies on the role of G-3-P in glycerolipid metabolic regulation have mostly been limited to regulatory interactions among metabolic pathways themselves. The G-3-P levels in chloroplasts were found to be a limiting factor for the secondary acylation step of the prokaryotic

pathway (39). It was further proposed that an elevated stroma G-3-P level stimulates the consumption of C16 onto the C-2-position of the 1-oleoyl glycerol-3-P, thereby controlling the chain elongation step of C16 to C18 fatty acid (39). Studies of the *gly1* mutant (25) have confirmed such a mode of metabolic action operating *in planta*. Our study revealed that the impact of G-3-P metabolic perturbation extends beyond the level of metabolite flux adjustment, and that it exerts control at the transcript level on enzymes of the two glycerolipid pathways. In addition to the general opposing trend of the two glycerolipid pathway, we find that ACP4 was one of the most induced genes in the $gpsA^{FR}$ line. The k_m of the chloroplast glycerol-3-phosphate acyltransferase for ACP-II in spinach, an otholog of the Arabidopsis ACP4, was shown to be 5 time less than ACP-I; whereas the thioesterase has much lower Km for ACP-I (40, 41). Hence, the preferential expression of ACP-4 is yet another contributing factor under the modulation of G-3-P that effected favorable partitioning of fatty acid to the prokaryotic pathway. Increases in the C16 level of glycerolipids of the $gpsA^{FR}$ line are in general agreement with the proposition that *in planta* the overall C16:C18 ratio is determined by competition between alternative pathways of C16:0 metabolism (15). However we observed that this chain length ratio change could also be partly explained by a modest reduction at the transcript level of KCS II (At1g74960), which was detected at 0.85 of that of the control. This reduction in KCS II on the one hand shifted the partitioning of lipid synthesis to the prokaryotic pathway as demonstrated in the *fab1* mutant (19), while on the other hand also reduced the elongation of 16:0 ACP to 18:0-ACP.

In summary, our study reveals a connection between G-3-P level changes and adjusted metabolic flux as well as altered gene expression of enzymes concerning glycerolipid metabolism in Arabidopsis. Given the current state of genomic and metabolic tools and resources, future studies will be possible to investigate if G-3-P is the *de facto* signal that turns up and down the transcription of genes or alterations in the dynamics of the lipid pathways instigated by G-3-P changes transduce signals to adjust gene expression.

Acknowledgments

The authors thank Dr. John E Cronan Jr for providing the Bacterial strain BB26-36R2 ($gpsA^{FR}$, *plsB*). We are grateful to Dr. Adrian Cutler, Mark Smith and Patrick Covello for critical reading of the manuscript and Dr. Wilf Keller and Dr. Faouzi Bekkaoui for project management. This

research was supported in part by the Saskatchewan Canola Development commission and the National Research Council Canada–Genomic and Health Initiatives, Genome Prairie, and Genome Canada, a not-for-profit organization that is leading Canada's national strategy on genomics. This research is National Research Council Canada Publication (XXXXX).

REFERENCES

1. Gardiner, S. E., Roughan, P. G., Slack, C. R. (1982) *Plant Physiol.* 70, 1316-1320
2. Ohlrogge, J., and Browse, J. (1995) *Plant Cell* 7, 957-970
3. Roughan, PG., and Slack, C. R. (1982) *Annu. Rev. Plant. Physiol.* 33, 97–132
4. Frentzen, M., Heinz, E., McKeon, T. A., Stumpf, P. K. (1983) *Eur. J. Biochem.* 129, 629-636
5. Heinz, E. (1977) Lipids and Lipid Polymers in Higher Plants (Telvini, M. &Lichtentaler, HK., eds), pp. 102-120, Springer-Verlag, Berlin, Heidelberg and New York
6. Heinz, E., Roughan, P. G. (1983) *Plant Physiol.* 72:273-279
7. Roughan, P. G., Holland, R., Slack, C. R. (1979) *Biochem. J.* 184, 571–574
8. Gardiner, S. E., Rough, P. G. (1983) *Biochem. J.* 210, 949-952
9. Schmidt, H., Heinz, E. (1993) *Biochem. J.* 289, 777-782
10. Browse, J., McCourt, P., and Somerville, C. (1986) *Plant Physiol.* 81, 859-864
11. Johnson, G., Williams, J. P. (1989) *Plant Physiol.* 91, 924-929
12. Brockman, J. A., Norman, H. A., Hilderbrand, D.F. (1990) *Phytochemistry* 29, 1447-1453
13. Härtel, H., Dörmann, P., and Benning, C. (2000) *PNAS* 97, 10649-10654
14. Browse, J., Warwick, N., Somerville, C., Slack, C. R. (1986) *Biochem. J.* 235, 25-31
15. Kunst, L., Browse, J., and Somerville, C. (1998) *PNAS* 85, 4143-4147
16. Browse, J., Kunst, L., Anderson, S., Hugly, S., Somerville, C. (1989) *Plant Physiol.* 90, 522-529
17. Kunst, L., Browse, J., and Somerville, C. (1989) *Plant Physiol.* 90, 943-947
18. Miquel, M., and Browse, J. (1992) *J. Biol. Chem.* 267, 1502-1509
19. Wu, J., James, Jr, D. W., Dooner, H. K., and Browse, J. (1994) *Plant Physiol.* 106, 143-150

20. Kachroo, P., Shanklin, J., Shah, J., Whittle, E. J., and Klessig, D. F. (2001) *PNAS* 98, 9448-9453
21. Kachroo, A., Lapchyk, L., Fukushige, H., Hildebrand, D., Klessig, D., and Kachroo, P. (2003) *Plant Cell* 15, 2952-2965
22. Kachroo, A., Venugopal, S. C., Lapchyk, L., Falcone, D., Hildebrand, D., and Kachroo, P. (2004) *PNAS* 101, 5152-5157
23. McKee, J. W., and Hawke, J. C. (1979) *Arch. Biochem. Biophys.* 197, 322-332
24. Roughan, P. G., Holland, R., Slack, C. R. (1980) *Biochem. J.* 188, 17-24
25. Miquel, M., Cassagne, C., Browse, J. (1998) *Plant Physiol.*117, 923-930
26. Bell, R. M., Cronan, Jr, J. E. (1975) *J. Biol. Chem.* 250, 7153-7158
27. Ou, X., Ji, C., Han, X., Zhao, X., Li, X., Mao, Y., Wong, L. L., Bartlam, M., Rao, Z. (2006) *J. Mol. Biol.* 357, 858-869
28. Fliege, R., Flügge, U. I., Werdan, K., Heldt, H. W. (1978) *Biochim. Biophys. Acta.* 502(2), 232-47
29. Falcone, D. L., Ogas, J. P., Somerville, C. (2004) *BMC Plant Biol.* 4, 17
30. Devaiah, S. P., Roth, M. R., Baughman, E., Li, M., Tamura, P., Jeannotte, R., Welti, R., and Wang, X. (2006) *Phytochemistry* 67(17), 1907-1924
31. Gentleman, R. C., Carey, V. J., Bates, D. M., Bolstad, B., Dettling, M., Dudoit, S., Ellis, B., Gautier, L., Ge, Y., Gentry, J., et al (2004) *Genome Biol.* 5, R80
32. Kelly, A. A., Froehlich, J. E., and Dörmann, P. (2003) *Plant Cell* 15: 2694-2706
33. Frentzen, M. (1993) Lipid Metabolism in Plants. Boca Raton, FL: CRC Press; pp. 195–231
34. Ghosh, S., Sastry, P.S. (1988) *Arch. Biochem. Biophys.* 262, 508–516
35. Shen, W., Wei, Y, Dauk, M., Tan, Y., Taylor, D. C, Selvaraj, G., and Zou, J. (2006) *Plant Cell* 18, 422-441
36. Wei, Y., Shen, W., Dauk, M., Wang, F., Selvaraj, G., Zou, J. (2004) *J Biol Chem.* 279(1), 429-35
37. Quettier, A. L., Shaw, E., Eastmond, P. J. (2008) *Plant Physiol.* 148(1), 519-528
38. Chanda, B., Venugopal, S. C., Kulshrestha, S., Navarre, D. A., Downie, B., Vaillancourt, L., Kachroo, A., and Kachroo, P. (2008) *Plant Physiol.* 147, 2017-2029
39. Sauer, A., and Heise, K. P. (1983) *Z. Naturforsch.* 38, 399-404

40. Guerra, D. J., Ohlrogge, J. B., and Frentzen, M. (1986) *Plant Physiol.* 82, 448-453
41. Bonaventure, G., and Ohlrogge, J. B. (2002) *Plant Physiol.* 128, 223-235
42. Bradford, M. M. (1976) *Anal. Biochem.* 72, 248–254
43. Ames, B. N. (1966) Methods Enzymol. 8, 115-118
44. Gautier, L., et al. (2004) *Bioinformatics* 20, 307–315
45. Bolstad, B. M., Irizarry, R. A., Astrand, M., and Speed, T. P. (2003) *Bioinformatics* 19(2), 185-193
46. Smyth, G. K. (2004) Statistical Applications in Genetics and Molecular Biology Vol. 3 : Iss. 1, Article 3
47. Benjamini, Y., and Hochberg, Y. (1995) Journal of the Royal Statistical Society, Series B (Methodological) 57 (1): 289–300.

Figure Legend

Figure 1a. Immunoblot analysis of gpsA^{FR} protein. Immunoblots of total leaf and chloroplast protein from the *gpsA*^{FR} transgenic and wild-type lines probed with polyclonal antiboies raised against two polypeptides from gpsA^{FR}. Lane 1: wild-type total leaf protein extract; lane 2: wild-type chloroplast protein extract; lane 3: total leaf protein extract from *gpsA*^{FR} transgenic line #84; lane 4: chloroplast protein extract from *gpsA*^{FR} transgenic line #84; lane 5: total leaf protein extract from *gpsA*^{FR} transgenic line #102-5; lane 6: chloroplast protein extract from *gpsA*^{FR} transgenic line #102-5; lane 7: total leaf protein extract from *gpsA*^{FR} transgenic line # 22-44; and lane 8: chloroplast protein extract from *gpsA*^{FR} transgenic line # 22-44. Approximately 10 μg of protein was loaded in each lane.

1b. G-3-P Contents of the *gpsA*^{FR} transgenic and wild-type (WT) Lines.
(A) G-3-P contents in leaves of *gpsA*^{FR} transgenic lines and wild type (WT) plants.
(B) G-3-P contents in chloroplast of *gpsA*^{FR} transgenic lines and wild type (WT) plants.

Figure 2. Fatty acid composition at the *sn*-2 position of leaf glycerolipids. A, MGDG; B: DGDG: C: PG; D: PC.

Figure 3a. Molecular species of DGDG, MGDG, and PG (mol% of total polar glycerolipids analyzed) in leaves of wild-type (WT) and *gpsA*^{FR} transgenic lines. Values are means ± SD ($n = 5$).

3b. Molecular species of PC, PE, and PI (mol% of total polar glycerolipids analyzed) in leaves of wild-type (WT) and *gpsA*^{FR} transgenic lines. Values are means ± SD ($n = 5$).

Figure 4. Schematic view of glycerolipid biosynthesis pathways integrated with microarray data. To visualize the relative transcript levels between *gpsA*^{FR} transgenic plants and wild type control, gene expression data were mapped to the pathway diagrams complied from AraCyc database (http://www.arabidopsis.org/biocyc/index.jsp) and Ohlrogge and Browse, 1995 and Kelly et al., 2003. Dash lines represent possible channeling between the ER and chloroplast. Red diamond represents induced genes, while green diamond denotes repressed genes based on transcript level ratio. ER, endoplasmic reticulum; oe, outer envelope; ie, inner envelope; FAS, fatty acid biosynthesis.

Figure 5. Real-time quantitative RT-PCR validation of microarray data. The relative expression levels of representative genes from microarray data as revealed by Real-time gene-expression analysis. Real-time qRT-PCR results using cDNA from WT (wild type, grey bar) and 22-44 (*gpsA*^{FR} transgenic line, black bar) as templates. For the comparison, the result from wild type control plants was normalized to 1 using StepOne software 2.0 (Applied Biosystems). Values represent the averages of three independent replicates.

A List of Supplemental Data

Supplemental Table S1. List of genes differentially expressed in *gpsA*^{FR} line.
Supplemental Table S2. List of genes complied from the Arabidopsis Lipid Gene Database.
Supplemental Table S3. List of genes used in the glycerolipid pathways.
Supplemental Table S4. List of genes used for microarray validation.
Supplemental Table S5. Primers used for real-time qRT-PCR

Table 1. Fatty Acid Composition of Total Leaf Lipids of *gpsA*^{FR} Transgenic Lines (15-6, 22-44, 54-8, 84-10 and 102-5) and wild-type Arabidopsis (WT). Values are expressed as means ± SD (n = 3). Double bond indices were calculated as described by Falcone et al (29)

	Fatty Acid Composition (mol %)									
	16:0	16:1	16:2	16:3	18:0	18:1	18:2	18:3	C16/C18	Doubl bond indice
WT	15.0 ± 0.3	3.9 ± 0.2	0.9 ± 0.1	12.6 ± 0.5	1.2 ± 0.1	3.1 ± 0.2	14.7 ± 0.3	48.6 ± 0.6	0.48	2.16
5-6	18.2 ± 0.8	3.8 ± 0.2	0.7 ± 0.6	22.6 ± 2.2	2.2 ± 0.3	0.9 ± 0.8	9.0 ± 0.1	42.4 ± 0.7	0.83	2.18
2-44	19.8 ± 1.6	3.2 ± 0.3	0.9 ± 0.1	18.0 ± 1.0	1.6 ± 1.0	2.2 ± 1.3	10.8 ± 0.8	43.5 ± 0.9	0.72	2.15
54-8	18.0 ± 0.9	2.9 ± 0.2	0.8 ± 0.1	17.8 ± 0.8	1.7 ± 0.3	1.2 ± 0.1	11.3 ± 0.7	46.3 ± 1.4	0.65	2.31
4-10	16.2 ± 0.3	3.6 ± 0.1	1.4 ± 0.1	23.0 ± 0.5	1.6 ± 0.1	1.5 ± 0.1	9.2 ± 0.3	43.5 ± 0.4	0.79	2.22
02-5	17.2 ± 0.4	3.1 ± 0.1	0.6 ± 0.5	21.1 ± 1.3	1.7 ± 0.1	0.7 ± 0.6	10.1 ± 0.6	45.6 ± 1.4	0.72	2.25

Table 2. Glycerolipid Profile and Fatty Acid Composition of leaf lipids from wild type (WT) and *gpsA*^{FR} transgenic lines (22-44 and 105-2). Values represent the average of three to five independent Samples.

Glycerolipid	Total Polar lipids	Fatty Acid Composition								
		16:0	16:1	16:2	16:3	18:0	18:1	18:2	18:3	C16/C18
	%	mol %								
MGDG										
WT	39.1	0.9	1.3	1.7	38.8	0.2	1.0	2.9	53.3	0.74
22-44	45.6	2.2	1.0	1.7	43.0	0.3	0.6	1.8	49.4	0.92
102-5	49.3	2.2	1.3	1.7	41.6	0.5	0.7	3.5	48.6	0.88
DGDG										
WT	17.1	14.6	0.3	0.7	3.0	1.2	0.9	4.9	74.4	0.23
22-44	13.3	25.0	0.4	1.0	5.1	2.6	0.9	4.8	60.2	0.46
102-5	14.9	24.0	0.5	0.9	4.4	2.5	1.2	5.4	61.1	0.43
SQDG										
WT	2.7	46.7				2.4	2.0	7.2	41.6	0.88
22-44	2.5	62.3				4.2	0.7	4.2	28.6	1.66
102-5	2.5	54.6				6.2	1.7	5.2	32.4	1.20
PG										
WT	11.7	30.2	26.8			1.1	4.9	9.9	27.1	1.32
22-44	12.8	42.0	26.5			2.8	3.2	5.4	20.1	2.18
102-5	13.8	35.4	28.4			2.6	4.0	6.8	22.8	1.77
PC										
WT	16.6	25.9				2.3	4.6	30.2	36.9	0.35
22-44	13.4	35.4				5.9	2.1	21.2	35.4	0.55
102-5	9.5	33.3				5.4	2.6	23.1	35.6	0.50
PE										
WT	9.6	32.9				2.1	3.3	34.6	27.2	0.49
22-44	9.6	38.4				3.5	1.0	26.1	30.9	0.62
102-5	8.4	36.7				5.2	1.4	27.6	29.0	0.58
PI										
WT	3.4	50.1				2.8	1.6	20.8	24.7	1.00
22-44	3.5	54.0				3.7	0.9	17.2	24.2	1.18
102-5	3.2	49.8				5.4	1.9	18.5	24.5	0.99

Table 3

	Mass of fatty acid (mol/100mol)	*sn*-2 position (%)		Flux to prokaryotic pathway (mol/1000 mol fatty acid)	Flux to eukaryotic pathway(mol/1000 mol fatty acid)
		C16	C18		
MGDG					
WT	391	72.3	27.7	283	108
22-44	456	84.7	15.3	386	70
102-5	493	82.8	17.2	408	85
DGDG					
WT	171	34.9	65.1	60	111
22-44	133	42.5	57.2	56	77
102-5	149	40.9	59.1	61	88
PG					
WT	117	63.9	36.1	75	42
22-44	128	66.9	33.1	86	42
102-5	138	81.7	18.3	112	26
PC					
WT	166	2.8	97.2	5	161
22-44	134	5.1	94.9	7	127
102-5	95	4.9	95.1	5	90

Comparison of fatty acid fluxes sharing in wild type (WT) and *gpsA*^{FR} lines (22-44, 102-5)

1. An original input of 1000 mol of fatty acids synthesized in the chloroplast as acyl-ACP species.
2. The tissue complement of each lipid was divided between the prokaryotic and eukaryotic pathway on the basis of content of C16 fatty acid at the *sn*-2 position.
3. The calculation was based on the results of Table 2 and Figure 2.

Figure 1.

A

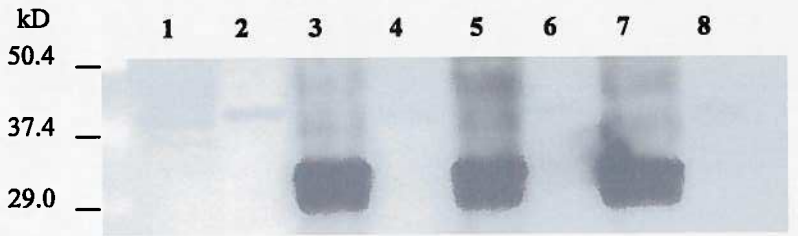
kD
1
2
3
4
5
6
7
8
50.4
37.4
29.0

B

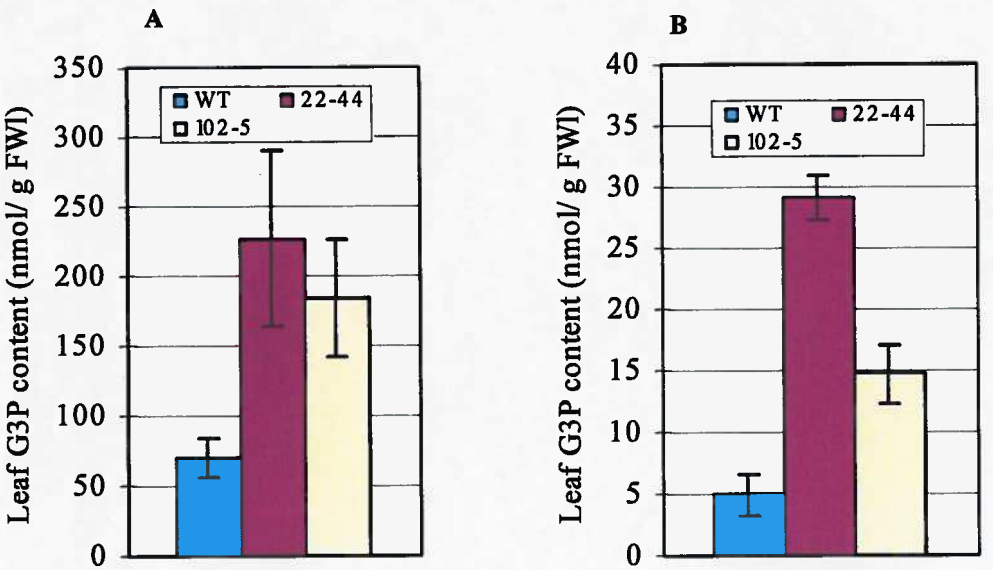
A
B
Leaf G3P content (nmol/ g FWl)
WT
22-44
102-5
350
300
250
200
150
100
50
0
40
35
30
25
20
15
10
5
0

Figure. 2

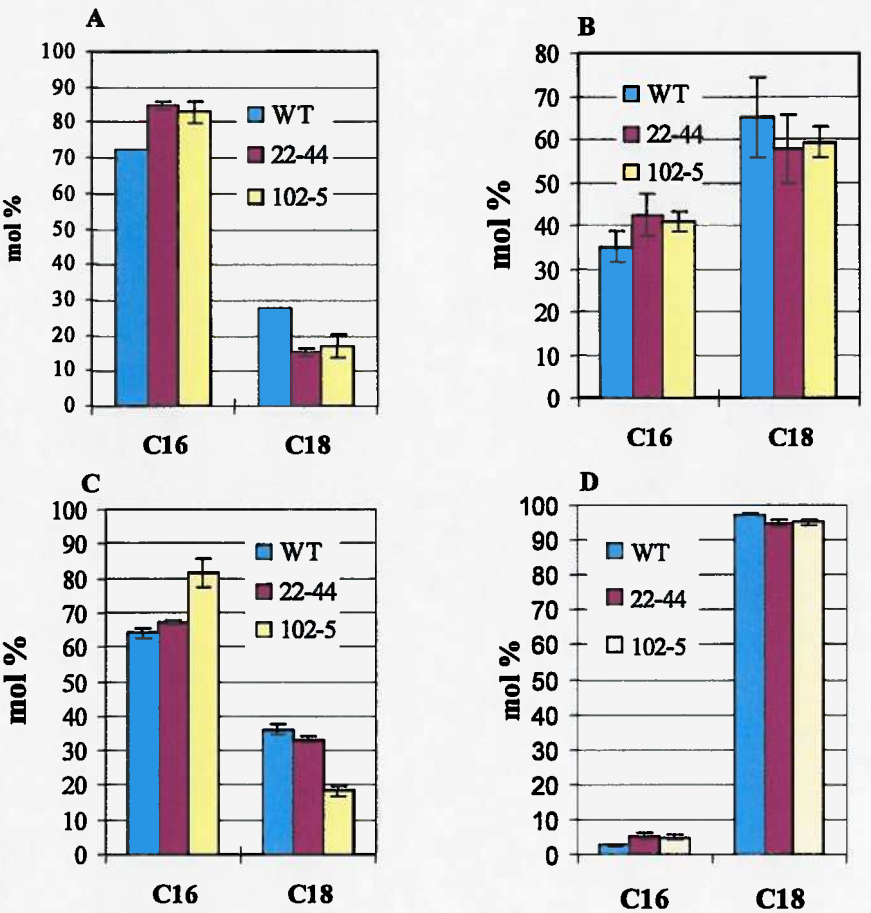

Figure 3

A

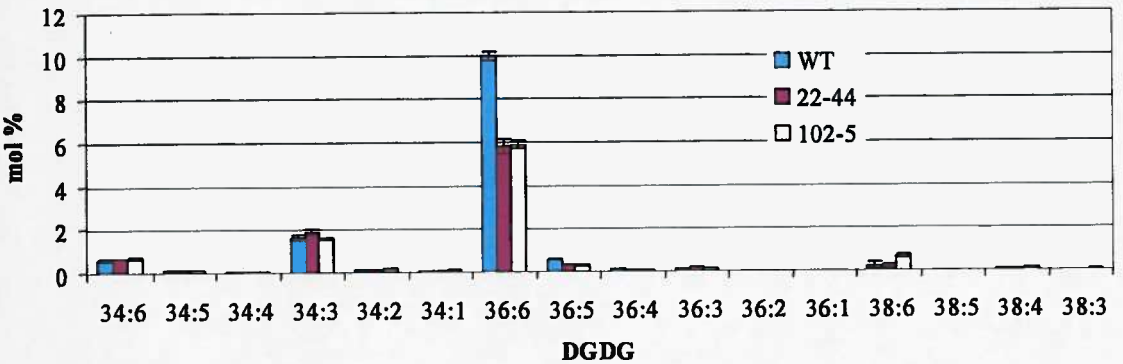
12
10
8
6
4
2
0
mol %
WT
22-44
102-5
34:6 34:5 34:4 34:3 34:2 34:1 36:6 36:5 36:4 36:3 36:2 36:1 38:6 38:5 38:4 38:3
DGDG

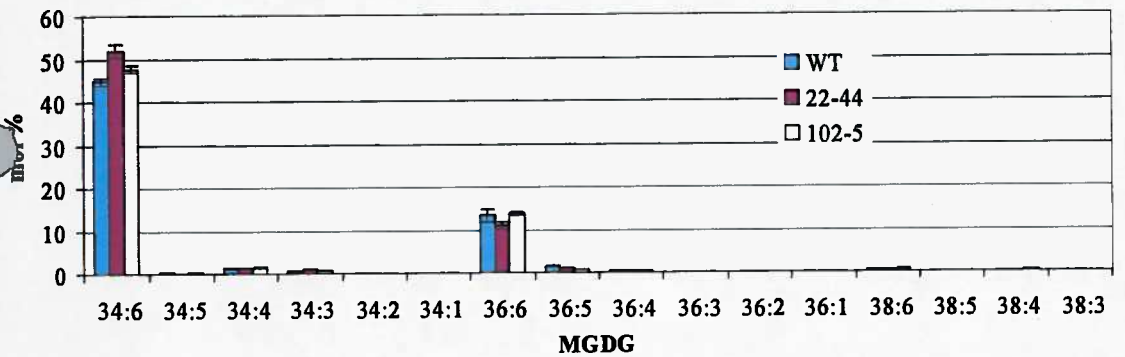
60
50
40
30
20
10
0
mol %
WT
22-44
102-5
34:6 34:5 34:4 34:3 34:2 34:1 36:6 36:5 36:4 36:3 36:2 36:1 38:6 38:5 38:4 38:3
MGDG

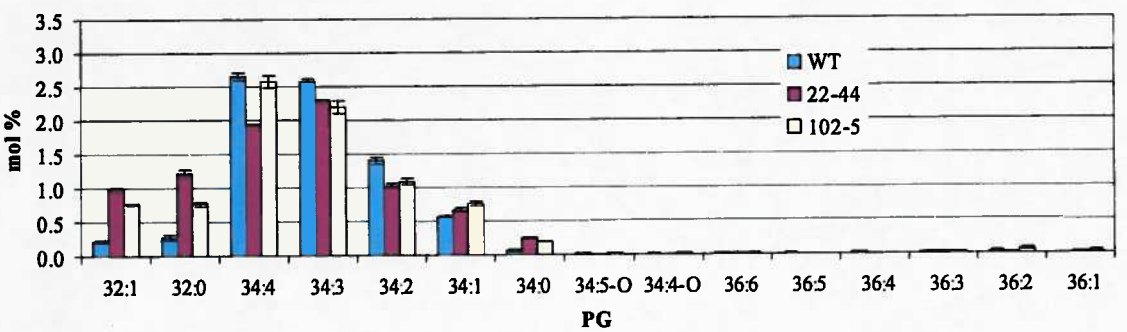
3.5
3.0
2.5
2.0
1.5
1.0
0.5
0.0
mol %
WT
22-44
102-5
32:1 32:0 34:4 34:3 34:2 34:1 34:0 34:5-O 34:4-O 36:6 36:5 36:4 36:3 36:2 36:1
PG

B

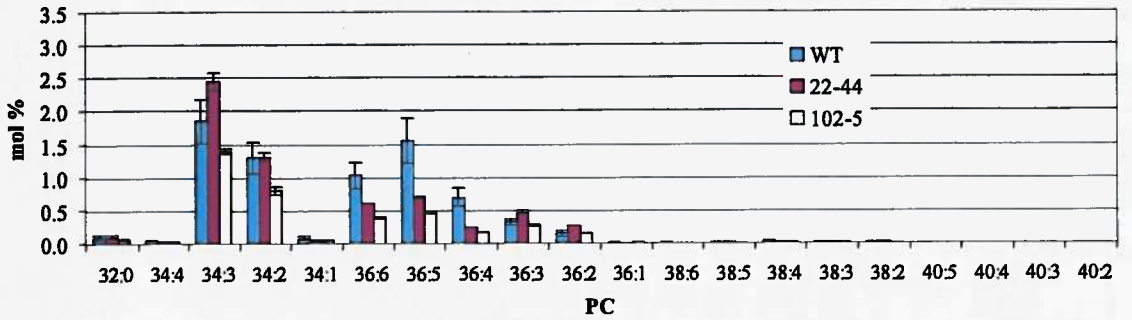
mol %
3.5
3.0
2.5
2.0
1.5
1.0
0.5
0.0
WT
22-44
102-5
32:0 34:4 34:3 34:2 34:1 36:6 36:5 36:4 36:3 36:2 36:1 38:6 38:5 38:4 38:3 38:2 40:5 40:4 40:3 40:2
PC

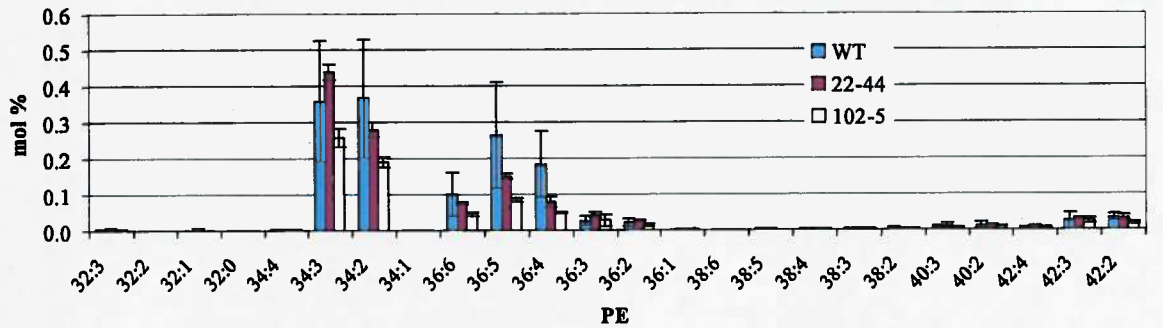
mol %
0.6
0.5
0.4
0.3
0.2
0.1
0.0
WT
22-44
102-5
32:3 32:2 32:1 32:0 34:4 34:3 34:2 34:1 36:6 36:5 36:4 36:3 36:2 36:1 38:6 38:5 38:4 38:3 38:2 40:3 40:2 42:4 42:3 42:2
PE

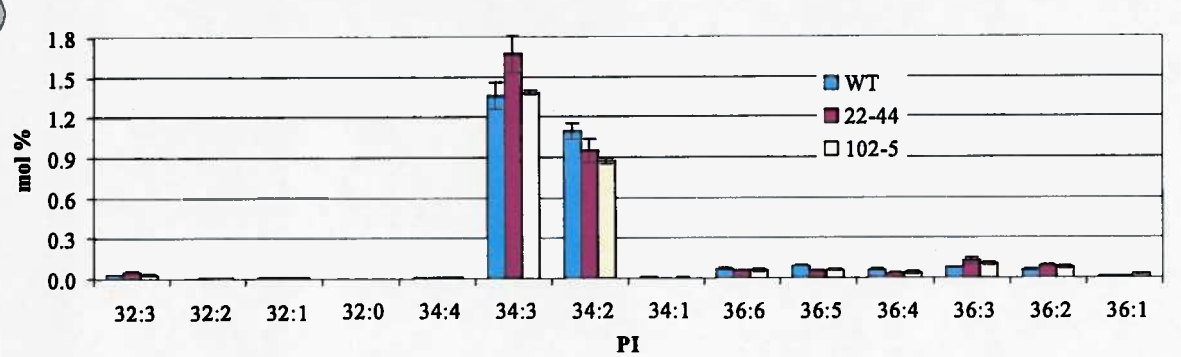
mol %
1.8
1.5
1.2
0.9
0.6
0.3
0.0
WT
22-44
102-5
32:3 32:2 32:1 32:0 34:4 34:3 34:2 34:1 36:6 36:5 36:4 36:3 36:2 36:1
PI

Figure 4

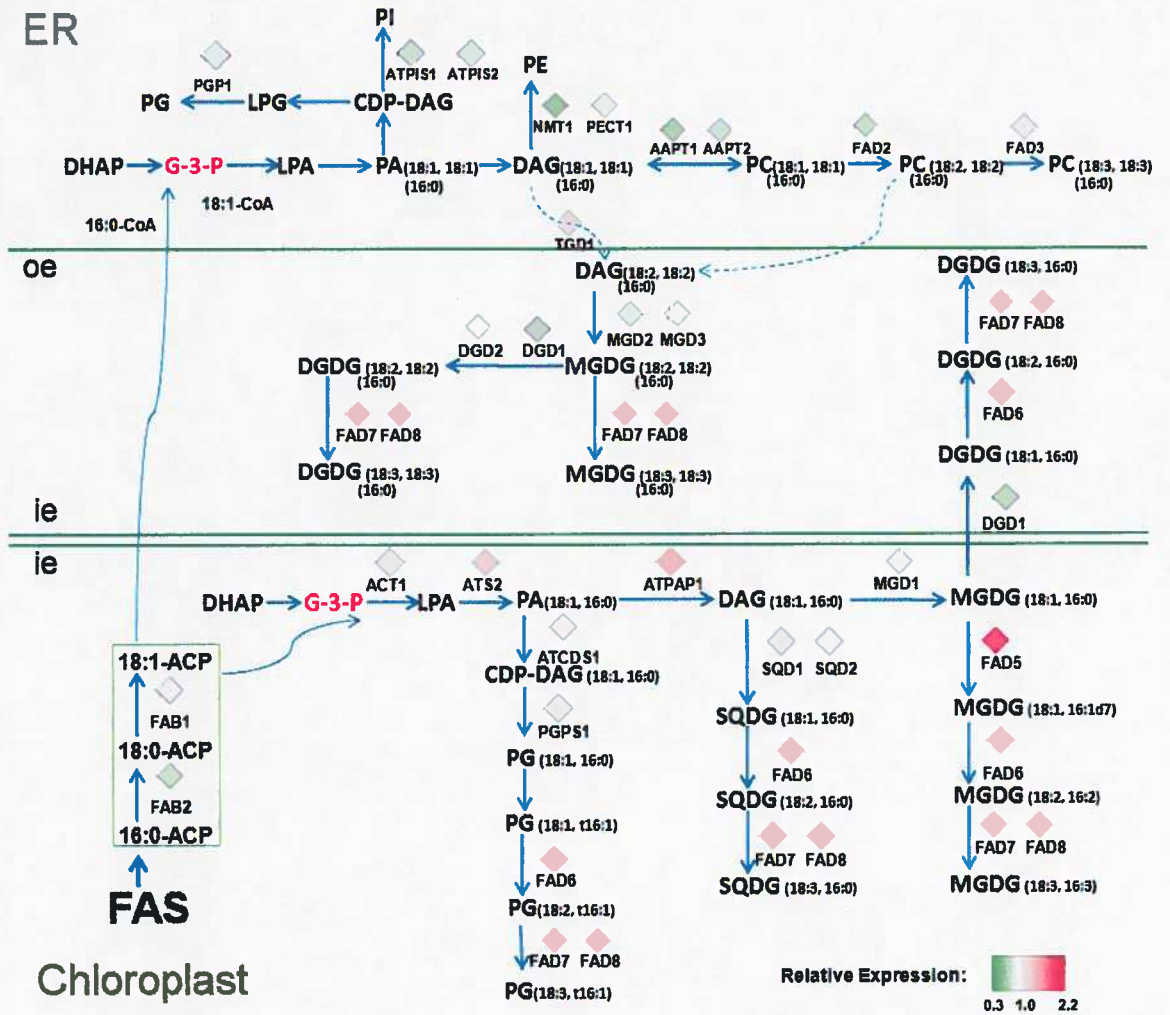
ER
PI
PE
PG
LPG
CDP-DAG
PGP1
ATPIS1
ATPIS2
NMT1
PECT1
DHAP
G-3-P
LPA
PA(18:1, 18:1) (16:0)
DAG(18:1, 18:1) (16:0)
AAPT1
AAPT2
PC(18:1, 18:1) (16:0)
FAD2
PC(18:2, 18:2) (16:0)
FAD3
PC(18:3, 18:3) (16:0)
18:1-CoA
16:0-CoA
TGD1
oe
DAG(18:2, 18:2) (16:0)
DGD2
DGD1
MGD2
MGD3
DGDG(18:2, 18:2) (16:0)
MGDG(18:2, 18:2) (16:0)
FAD7 FAD8
DGDG(18:3, 18:3) (16:0)
MGDG(18:3, 18:3) (16:0)
DGDG(18:3, 16:0)
DGDG(18:2, 16:0)
DGDG(18:1, 16:0)
FAD6
DGD1
ie
ie
ACT1
ATS2
ATPAP1
MGD1
PA(18:1, 16:0)
DAG(18:1, 16:0)
MGDG(18:1, 16:0)
18:1-ACP
FAB1
18:0-ACP
FAB2
16:0-ACP
FAS
Chloroplast
ATCDS1
CDP-DAG(18:1, 16:0)
PGPS1
PG(18:1, 16:0)
PG(18:1, t16:1)
PG(18:2, t16:1)
PG(18:3, t16:1)
SQD1
SQD2
SQDG(18:1, 16:0)
SQDG(18:2, 16:0)
SQDG(18:3, 16:0)
FAD5
MGDG(18:1, 16:1d7)
MGDG(18:2, 16:2)
MGDG(18:3, 16:3)
Relative Expression:
0.3 1.0 2.2

Figure 5

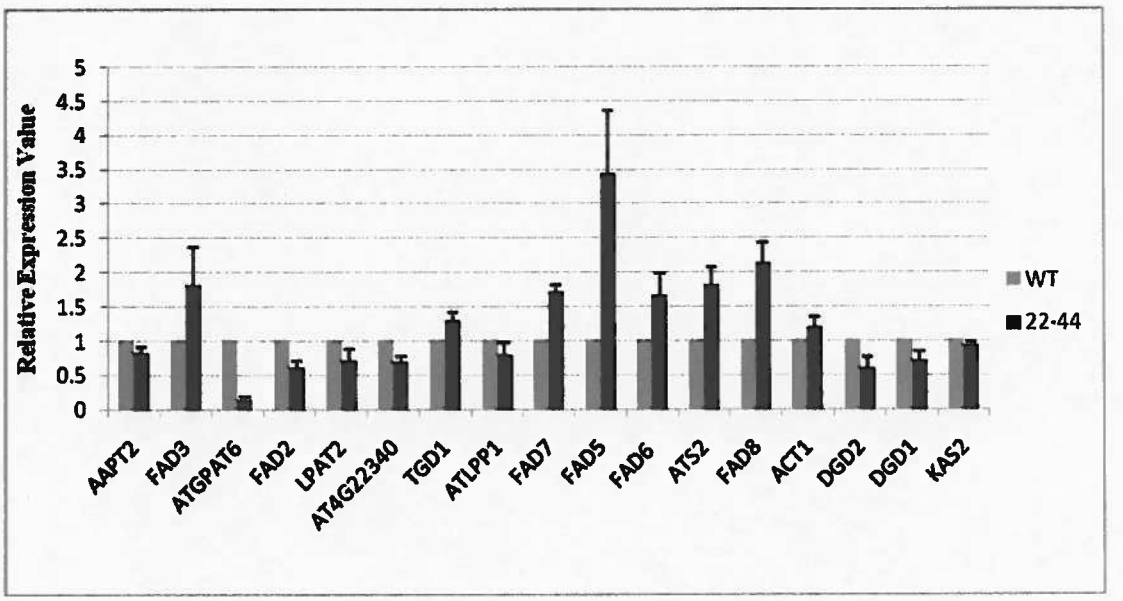
Relative Expression Value
5
4.5
4
3.5
3
2.5
2
1.5
1
0.5
0
WT
22-44
AAPT2
FAD3
ATGPAT6
FAD2
LPAT2
AT4G22340
TGD1
ATLPP1
FAD7
FAD5
FAD6
ATS2
FAD8
ACT1
DGD2
DGD1
KAS2